VOL. 10, NO. 6, APRIL 2015 ISSN 1819-6608

ARPN Journal of Engineering and Applied Sciences



www.arpnjournals.com

# DESIGN AND SIMULATION OF VOLTAGE BOOSTER CIRCUIT USING COUPLED INDUCTOR

P. Muthukrishnan[1] and R. Dhanasekaran[2]

[1]St.Peter's University, Chennai, TN, India

[2]Syed Ammal Engineering College, Ramanathapuram, TN, India

E-Mail: pmk.12345@gmail.com

## ABSTRACT

In this paper, a high voltage gain of DC-DC converter with design and simulation are proposed using coupled-inductor. The proposed converter duty ratio is 0.65, so appropriate duty ratio is considering for this design of the converter. Due do more number of switches are considers for the converter circuit will make more switching power losses but in this converter using only two switches and have low voltage stress across power switches. The recycling processes are takes place in the coupled inductor, because of this energy stored in leakage inductor. The steady-state analyses and the operating principles with modes of operations of proposed converter are discussed properly in below detail. Finally the proposed converter design and simulation output are obtained in terms of output voltage is 271 voltages from the input of 24 voltage of the DC battery supply and output power of 407W and efficiency is 96.6% in designed and simulated using MATLAB/ SIMULINK.

**Keywords:** coupled inductor, leakage inductor, operating modes, renewable energy and voltage booster.

## INTRODUCTION

Theoretically, conventional step-up converters such as the support converter and flyback converter can't accomplish a high venture up transformation with high proficiency in light of the resistances or leakage inductance. Hence a changed boost–flyback converter was anticipated and numerous converters are utilized the coupled inductor for a respectably high voltage transformation level (P.Muthukrishnan *et al.* 2014).

To achieve a high step-up voltage ratio, transformer- and coupled-inductor-based converters are usually the right choices. Compared with an isolation transformer, a coupled inductor has a simpler winding structure, lower conduction loss, and continuous conduction current at the primary winding, resulting in a smaller primary winding current ripple and lower input filtering capacitance (P.Muthukrishnan *et al.* P.Muthukrishnan *et al.* 2014, 2013).

The duty cycle of a dc–dc transformer, which is an open-loop controlled isolated dc–dc converter, is fixed at 50%. As a result, soft switching of all the power switches can be always achieved by utilizing the leakage or magnetizing inductance (Hongfei Wu *et al.* 2015).The large duty ratios, high switch voltage stresses, and serious output diode reverse recovery problem are still major challenges for high step up and high power conversion with satisfactory efficiency (Xuefeng Hu *et al.* 2015).

High step-up ratio can be achieved by combining classical boost converter with switched inductors (Longlong Zhang, *et al.* 2015). The converter with fuel cell input source is suitable to operate in continuous conduction mode (CCM) because the discontinuous conduction mode operation results in large input current ripple and high peak current, which make the fuel cell stacks difficult to afford (Kuo-Ching Tseng *et.al*, MehnazAkhter Khan *et al.* 2015, 2014).

The dc-bias of magnetizing current in the magnetic core, leading to smaller sized magnet. Since the magnetizing current has low dc-bias, the ripple magnetizing current can be utilized to assist ZVS of main switch, (Bin Gu, Jason Dominic *et al.* 2015)while maintaining low root mean- square (RMS) conduction loss. The prototype presents low size and volume because magnetic are designed for twice the switching frequency. In addition, good efficiency results over the entire load range (George Cajazeiras Silveira *et al.* 2014),i.e., higher than 92% .However, electricity produced by these renewable energy sources is changing irregularly due to the natural environment and the climate change. For example, a photovoltaic power system is particularly susceptible to weather condition and location (Jae-Won Yang et.al, Luiz Henrique S *et al.* 2014, 2014), the converter can generate a dc bus with a battery bank or a photovoltaic panel array, allowing the simultaneous charge of the batteries according to the radiation level (Fatih Evran *et al.* 2014).

The high step-up ratio dc–dc converters are chosen in solar energy systems. A low duty ratio is recommended in this paper. The coupled inductor leakage inductance energy can efficiently be discharged (Jiarong Kan,Shaojun Xie *et al.* 2014).

## PROPOSED CONVERTER

The proposed converter circuit configuration are consists of two active switches $S_1$and $S_2$, one coupled inductor, three diodes $D_1$, $D_2$ and$D_3$ and then two output capacitors $C_1$and $C_2$are the switching element. The actual circuit of the proposed converter is shown in Figure-1. The coupled inductor magnetizing components are in a magnetizing inductor $L_m$, primary leakage inductor $L_{k1}$, secondary leakage inductor $L_{k2}$.

VOL. 10, NO. 6, APRIL 2015 ISSN 1819-6608
ARPN Journal of Engineering and Applied Sciences

www.arpnjournals.com

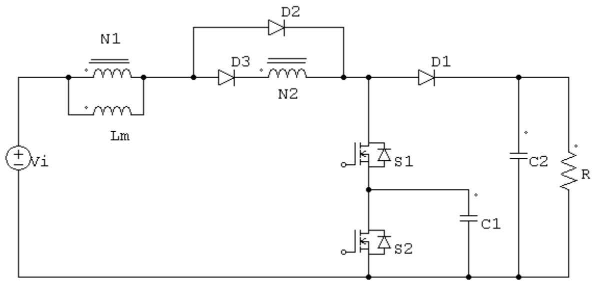


**Figure-1.** The circuit diagram of proposed converter.

The assumptions are considered the circuit analyses of the proposed converter. All components are ideal in the First consideration and the $R_{DS}$(ON) on-state resistance of the active switches, forward voltage drop on diodes & the ESR (equivalent series resistance) of the coupled-inductor and output capacitors are neglects. The coupled inductor turn's ratio is equal to $N_2/N_1$. The operation of four modes are explains in below section and all mode of operation of full circuit function are explained in Figure-2.

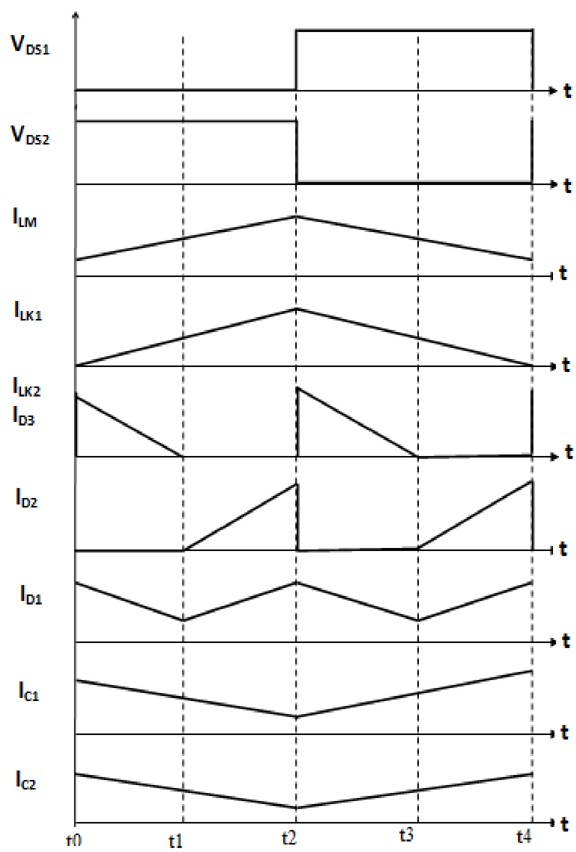


**Figure-2.** The function of proposed converter in all the modes.

**Mode 1 [$t_o$, $t_1$]:** In this mode consider as $S_1$is turned on and $S_2$ is turned off, diodes $D_3$ and $D_1$ are conducting and $D_2$ is not conducting. The DC-source energy is transferred to $L_m$ and $L_{k1}$through $D_3$, $D_1$, and $S_1$, so currents $i_{Lm}$, $i_{Lk1}$ and $i_{D3}$are same and also increasing up to maximum level of $i_{Lm.}$ The current-flow path is shown in Figure-3. The secondary leakage inductor current $i_{lk2}$is declined according to $i_{LM}/n$. This mode ends when the increasing $i_{lk1}$ equals the decreasing $i_{Lm}$ and this is equal to $V_i\times N_2/N_1$.In addition, $D_1$ becomes forward-biased; $C_2$ is charged to $V_i + V_o\times N_2/N_1$ The energy stored in $L_{k2}$is released to $C_1$,$C_2$ and Load through $S_1$ and $D_1$, so the capacitor $C_1$ is increasing the energy at the same time the energies stored in $C_2$are discharged to the load

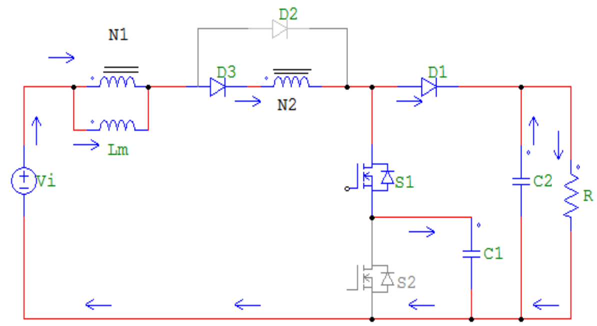


**Figure-3.** The current flow path in Mode I.

**Mode 2 [$t_1$, $t_2$]:** During this interval, $S_1$is still turned on and $S_2$is turned off and diode $D_2$ and $D_1$ are turned on and $D_3$ is turned off because of some energy decreased in $i_{Lk2.}$ The current-flow path is shown in Figure-4. The DC source, $L_m$, and $L_{k1}$are series-connected to transfer their energies to $L_{k2}$, $C_1$ and also input voltage $V_i$ is imposed on $N_1$, thus causing $L_m$ to be magnetized and the voltage across $N_2$to be induced, equal to $V_i\times N_2/N_1$. In addition, $D_1$ becomes forward-biased; C2 is charged to $V_i+ V_o\times N_2/N_1$. Thus, $i_{Lm}$ and $i_{Lk1}$are decreased. The leakage inductor ($L_{k1}$)stored energy is recycled to $C_1$. The Capacitor $C_2$stored energy is continuously discharged to the load.

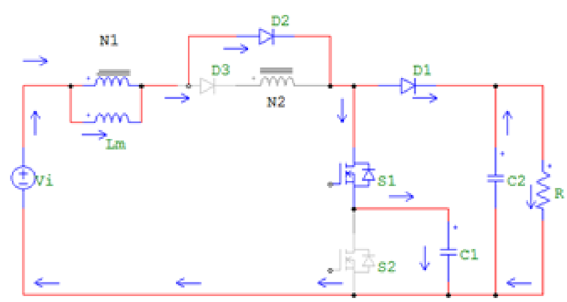


**Figure-4.** The current flow path in Mode II.

**Mode 3 [$t_2$, $t_3$]:**In this mode, $S_1$is consider as off and $S_2$is consider as on and diodes $D_{3,}$ $D_1$ are turned on and $D_2$ is off. The dc-battery energy is moved to $L_m$ and $L_{k1}$ over $D_3$ and $S_2$. The currents $i_{Lm}$, $i_{Lk1}$, $i_{D3}$ are improved. The $L_{k2}$energy stored is released to $C_2$, $C_1$ over $S_2$. The decreasing in $i_{Lk1}$. The $L_{k1}$and$C_1$energy is recycled. The

VOL. 10, NO. 6, APRIL 2015 ISSN 1819-6608

ARPN Journal of Engineering and Applied Sciences



www.arpnjournals.com

energies stored in $C_2$are discharged to the load. The current-flow path is shown in Figure-5. This mode ends when $i_{D2}$is higher than$i_{Lk2}$. In this mode the circuit current flows is still directed to the output terminal, but the magnitudes of current decreases gradually.

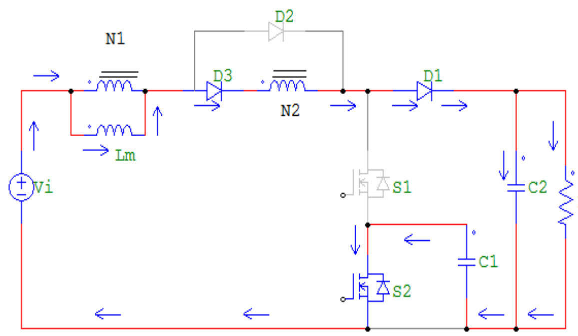


**Figure-5.** The current flow path in Mode III.

**Mode 4 [$t_3$, $t_4$]:** In this mode, $S_1$is still turned off and $S_2$is still turned on and diode $D_2$ and $D_1$ are turned on and $D_3$ is turned off. The DC source, $L_m$ and $L_{k1}$are series-connected to transfer their energies to $C_{2,}$ $C_1$ and the load. Thus $i_{Lm}$ and$i_{Lk1}$are decreased. The energy stored in $C_2$is still discharged to the load. The current-flow path is shown in Figure-6. In this mode the circuit current flows is still directed to the output terminal, but the magnitudes of current $I_{c1}$ decreases gradually.

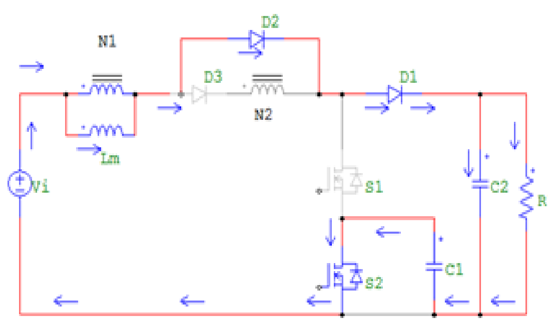


**Figure-6.** The current flow path in Mode IV.

## CONVERTERSTEADY STATE ANALYSIS

### The CCM operation

The steady state analysis is simplified by two modes. At CCM operation, the mode 1 and 2 giving the following equations:

$$V_{L1}^{I} = V_{L1}^{II} = kV_{in} \tag{1}$$

Where the coupled-inductor coupling-coefficient k is equal to $\frac{L_m}{(L_m+L_{k1})}$

The following mode 2 equations:

$$V_{in} - V_{c1} - V_{c2} = V_{L1}^{II} + V_{Lk1}^{II} \tag{2}$$

$$v_{Lk1}^{II} = L_{k1}\frac{di_{Lk1}^{II}}{dt} = n^2 L_{k1}\frac{di_{Lk1}^{II}}{dt} n^2 v_{Lk1}^{II} \tag{3}$$

Sub (3) into (2)

$$V_{in} - V_{c1} - V_{c2} = (1+n)V_{L1}^{II} + (1+n^2)V_{Lk1}^{II} \tag{4}$$

Voltage $v_{L1}^{II}$ is written as,

$$v_{L1}^{II} = L_m\frac{di_{Lm}^{II}}{dt} = (1+n)L_m\frac{di_{Lk1}^{II}}{dt} \tag{5}$$

$$v_{Lk1}^{II} = L_{k1}\frac{di_{Lk1}^{II}}{dt} = \frac{L_{k1}}{(1+n)L_m}v_{L1}^{II} = \frac{1-k}{(1+n)k}v_{L1}^{II} \tag{6}$$

Sub (6) into (4)

$$v_{L1}^{II} = \frac{(1+n)k}{1+2nk+n^2}(V_{in} - V_{c1} - V_{c2}) \tag{7}$$

$$\frac{di_{Lm}^{II}}{dt} = \frac{(1+n)k}{1+2nk+n^2} \times \frac{V_{in}-V_{c1}-V_{c2}}{L_m} \tag{8}$$

The voltage across $L_m$ at mode IV

$$v_{L1}^{IV} = \frac{(1+n)k}{1+2nk+n^2}(V_{in} - V_{c1} - V_{c2}) \tag{9}$$

$$\frac{di_{Lm}^{IV}}{dt} = \frac{(1+n)k}{1+2nk+n^2} \times \frac{V_{in}-V_{c1}-V_{c2}}{L_m} \tag{10}$$

The volt-second balance principles are:

$$2\int_0^{\frac{DT_S}{2}} V_{L1}^{I}dt + 2\int_0^{\frac{(1-D)T_S}{2}} V_{L1}^{IV}dt = 0 \tag{11}$$

From above steps, voltage gain is obtained as

$$M_{CCM} = \frac{V_o}{V_{in}} = \frac{2(1+n-nD+n^2D+2nDk)}{(1-D)(1+n)} \tag{12}$$

If the neglected value of leakage inductor of the coupled inductor, so the coupling coefficient k is equal to 1. Substituting the above equation as,

$$M_{CCM} = \frac{V_o}{V_{in}} = \frac{2(1+nD)}{1-D} \tag{13}$$

ARPN Journal of Engineering and Applied Sciences

www.arpnjournals.com

## DESIGN PARAMETERS OF CONVERTER

The component design parameters are determined the following condition.

### The coupled inductor design

The coupled inductor is showed as a ideal transformer, a leakage inductor ($L_{k1}$)n, the magnetizing inductor ($L_m$) and The turns ratio (n) and the coupling coefficient (K) is ideal transformer are defined as

$$K = \frac{L_m}{L_m + L_k} \tag{14}$$

So, k=1, the following equations using this values

$$L_1 = \frac{nD(1-D)R}{2+(2+nD)} \tag{15}$$

$$\frac{L_1}{L_2} = \frac{N_2}{N_1} \tag{16}$$

$$L_m = \frac{D(1-D)2R}{2(n+2)(2+nD)f} \tag{17}$$

From equation (14), (15), (16) and (17) choice the values $L_1$=8mH, $L_2$=8mH, and $L_m$=2mH

### Designing the capacitors

$$C_1 = \frac{I_S(1-D)}{fvs} \tag{18}$$

$$C_2 = \frac{I_O D(1-D)}{fvs} \tag{19}$$

Choice the value of capacitor $C_1$ & $C_2$=5µf. The design parameters of proposed converter are given Table-1.

**Table-1.** Design parameters of proposed system.

| S. No. | Parameters | Values |
|---|---|---|
| 1 | Input voltage | 24V |
| 2 | Capacitor ($C_1$& $C_2$) | 5µF |
| 3 | Switching frequency | 50KHZ |
| 4 | Load resistance | 180Ω |
| 5 | Turn's ratio ($n_1$:$n_2$) | 1:2 |
| 6 | Inductor $L_1$,$L_2$, $L_m$ | 8mH,8mH, 2mH |
| 7 | Duty cycle | 0.65 |
| 8 | Output voltage | 271V |
| 9 | Output Current | 1.5A |
| 10 | Output power | 407W |

## EFFICIENCY CALCULATION

The efficiency is calculated by the total power out divided by total power into the circuit. The Calculate efficiency at full load condition by calculate the input power and output power

Efficiency in percentage

= (Output Power/Input Power)*100

The output power at load

$$P_0 = V_0 * I_0$$

$$P_0 = 271*1.5$$

$$P_0 = 407W$$

Input power

$$P_{in} = V_{in} * I_{in}$$

$$P_{in} = 24*17.5$$

$$P_{in} = 420W$$

Efficiency

$$\eta = \frac{407}{420}*100$$

$$\eta = 96.9\%$$

So we get better efficiency at load condition that is 96.9%

## RESULTS AND DISCUSSIONS

In this paper discussed the design and simulation of voltage booster Converter with Coupled Inductor. The proposed converter duty ratio is 0.65, so appropriate duty ratio is considering for this design of the converter. Obtain a more voltage gain with good design of the boost converter circuit. The coupled inductor are utilized the wastage of leakage energy is recycled in same converter circuit. The simulation diagram of Resistive load in the Figure-7, the input voltage and Input Current waveforms are in Figure-8 and Figure-9 and the output voltage & output current waveforms are in Figure-10 and Figure-11.The Output Voltage variation & Output Current variation with short duration waveforms are in Figure-12 and Figure-13 are discussed in this paper.

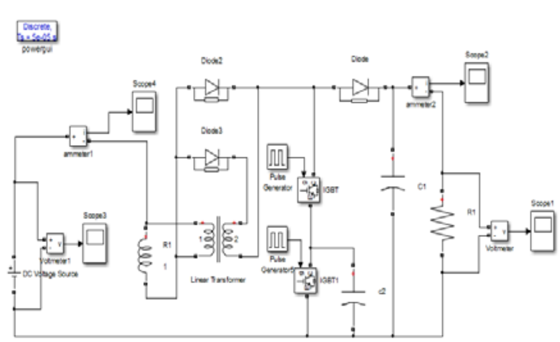

**Figure-7.** The simulation diagram of resistive load.

ARPN Journal of Engineering and Applied Sciences



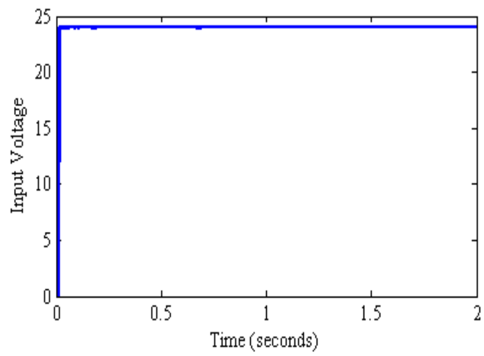


**Figure-8.** The input voltage waveform.

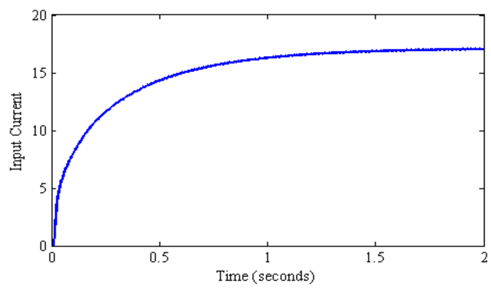


**Figure-9.** The Input Current waveform.

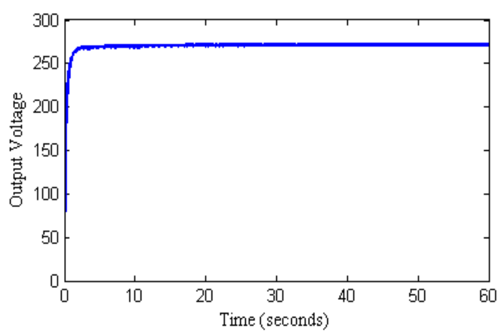


**Figure-10.** The output voltage waveform.

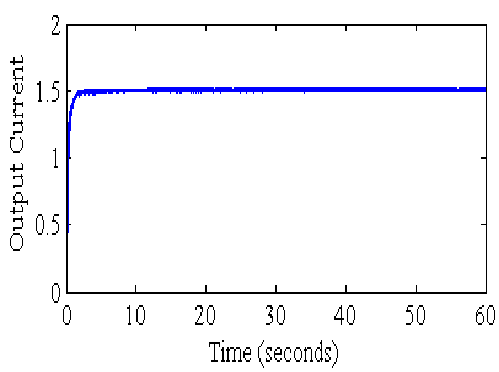


**Figure-11.** The output current waveform.

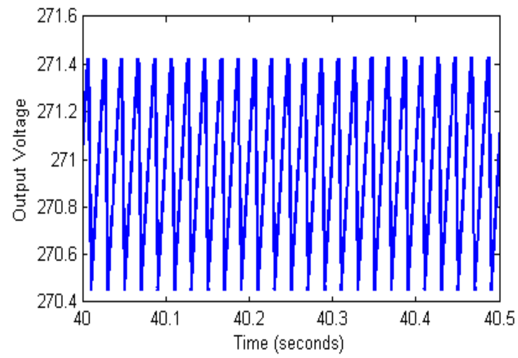


**Figure-12.** Output Voltage variation with short duration.

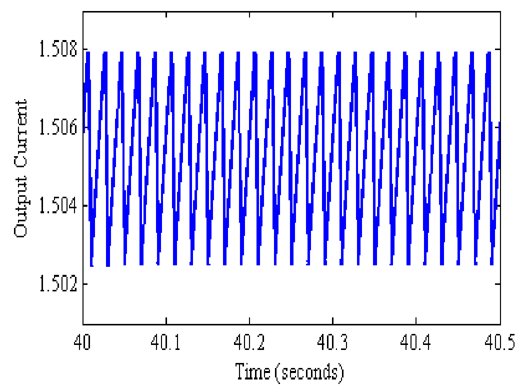


**Figure-13.** Output Current variation with short duration.

## CONCLUSIONS

The proposed converter design and simulation of voltage boost circuit using coupled inductor for obtained the high gain DC-DC converter are presented in this paper. The coupled-inductor with supporting of two capacitor and two switches possible of obtained high voltage gain. The coupled inductor is the major role of energy stored in the leakage inductor can be recycled. Finally, a simulation circuit for the proposed boost converter with 24-V input voltage from the battery, output voltage of 271V, and the output power of 407W, the actual efficiency is 96.9% at the full-load for the simulation using MATLAB/ SIMULINK.

## REFERENCES

[1] P. Muthukrishnan and R. Dhanasekaran. 2014. A High Step-Up Converter with a Voltage Multiplier & Coupled Inductor Module for Photovoltaic System. IEEE International Conference on Advanced Communication, Control & Computing Technologies, pp. 1041-1045, May.

ARPN Journal of Engineering and Applied Sciences





[2] P. Muthukrishnan and R. Dhanasekaran. 2014. Dc-Dc Boost Converter For Solar Power Application. Journal of Theoretical and Applied Information Technology Vol. 68 No.3, pp. 630-636, October.

[3] P. Muthukrishnan and R. Dhanasekaran. Simulation of DC- DC Boost Converter by Coupled Inductor Using PSIM," International Journal of Recent Development in Engineering and Technology Volume 1, Issue 1, pp. 25-30, October.

[4] Hongfei Wu, Yangjun Lu, Tiantian Mu, and Yan Xing. A Family of Soft-Switching DC–DC Converters Based on a Phase-Shift-Controlled Active Boost Rectifier. IEEE Transactions On Power Electronics, Vol. 30, No. 2, pp. 657-667, February.

[5] Xuefeng Hu and Chunying Gong. 2015. A High Gain Input-Parallel Output-Series DC/DC Converter With Dual Coupled Inductors," IEEE Transactions On Power Electronics, Vol. 30, No. 3, pp. 1306-1317, March.

[6] Longlong Zhang, Dehong Xu, Guoqiao Shen, Min Chen, Adrain Ioinovici and Xiaotian Wu. 2015. A High Step-Up DC to DC Converter Under Alternating Phase Shift Control for Fuel Cell Power System," IEEE Transactions On Power Electronics, Vol. 30, No. 3, pp. 1694-1703, March.

[7] Kuo-Ching Tseng, Jang-Ting Lin and Chi-Chih Huang. 2015. High Step-Up Converter With Three-Winding Coupled Inductor for Fuel Cell Energy Source Applications," IEEE Transactions On Power Electronics, Vol. 30, No. 2, pp.574-581, February.

[8] Bin Gu, Jason Dominic, Baifeng Chen, Lanhua Zhang. and Jih-Sheng Lai. 2015. Hybrid Transformer ZVS/ZCS DC–DC Converter With Optimized Magnetics and Improved Power Devices Utilization for Photovoltaic Module Applications. IEEE Transactions On Power Electronics, Vol. 30, No. 4, pp. 2127-2136, April.

[9] Mehnaz Akhter Khan, Iqbal Husain and Yilmaz Sozer. 2014. A Bidirectional DC–DC Converter With Overlapping Input and Output Voltage Ranges and Vehicle to Grid Energy Transfer Capability. IEEE Journal Of Emerging And Selected Topics In Power Electronics, Vol. 2, No. 3, pp. 507-516, September.

[10] George Cajazeiras Silveira, Fernando Lessa Tofoli, Luiz Daniel Santos Bezerra and René Pastor Torrico-Bascopé. 2014. A Nonisolated DC–DC Boost Converter With High Voltage Gain and Balanced Output Voltage. IEEE Transactions On Industrial Electronics, Vol. 61, No. 12, pp. 6739-6746, December.

[11] Jae-Won Yang and Hyun-Lark Do. 2014. High-Efficiency Bidirectional DC–DC Converter With Low CirculatingCurrent and ZVS Characteristic throughout a Full Range of Loads. IEEE Transactions On Industrial Electronics, Vol. 61, No. 7, pp. 3248-3256, July.

[12] Luiz Henrique S. C. Barreto, Paulo Peixoto Prac¸a, Demercil S. Oliveira Jr. and Ranoyca N. A. L. Silva. 2014. High-Voltage Gain Boost Converter Based on Three-State Commutation Cell for Battery Charging Using PV Panels in a Single Conversion Stage" IEEE Transactions On Power Electronics, Vol. 29, No. 1, pp. 150-158, January.

[13] Fatih Evran and Mehmet Timur Aydemir. 2014. Isolated High Step-Up DC–DC Converter With Low Voltage Stress," IEEE Transactions On Power Electronics, Vol. 29, No. 7, pp. 3591-3603, July.

[14] Jiarong Kan, Shaojun Xie, Yu Tang and Yunya Wu. 2014. Voltage-Fed Dual Active Bridge Bidirectional DC/DC Converter With an Immittance Network. IEEE Transactions On Power Electronics, Vol. 29, No. 7, pp. 3582-3590, July.